MANUFACTURING AUTOMATION

METAL CUTTING MECHANICS, MACHINE TOOL VIBRATIONS, AND CNC DESIGN

YUSUF ALTINTAS

University of British Columbia

CAMBRIDGE UNIVERSITY PRESS

PUBLISHED BY THE PRESS SYNDICATE OF THE UNIVERSITY OF CAMBRIDGE
The Pitt Building, Trumpington Street, Cambridge, United Kingdom

CAMBRIDGE UNIVERSITY PRESS
The Edinburgh Building, Cambridge CB2 2RU, UK http://www.cup.cam.ac.uk
40 West 20th Street, New York, NY 10011-4211, USA http://www.cup.org
10 Stamford Road, Oakleigh, Melbourne 3166, Australia
Ruiz de Alarcón 13, 28014 Madrid, Spain

© Cambridge University Press 2000

This book is in copyright. Subject to statutory exception
and to the provisions of relevant collective licensing agreements,
no reproduction of any part may take place without
the written permission of Cambridge University Press.

First published 2000

Printed in the United States of America

Typeface Century Schoolbook 10/13 pt. and Univers *System* LaTeX 2$_\varepsilon$ [TB]

A catalog record for this book is available from the British Library.

Library of Congress Cataloging in Publication Data
Altintas, Yusuf, 1954–
Manufacturing automation : metal cutting mechanics, machine tool vibrations, and CNC design / Yusuf Altintas.
p. cm.
ISBN 0-521-65029-1 (hc.). – ISBN 0-521-65973-6 (pbk.)
1. Machining – Automation. 2. Machine-tools – Vibration.
3. Machine-tools – Numerical control. I. Title.
TJ1185.5.A48 2000
671.3′5 – dc21 99-30935
CIP

ISBN 0 521 65029 1 hardback
ISBN 0 521 65973 6 paperback

CONTENTS

CHAPTER TWO

MECHANICS OF METAL CUTTING

2.1 INTRODUCTION

The final shapes of most mechanical parts are obtained by machining operations. Bulk deformation processes, such as forging and rolling, and casting processes are mostly followed by a series of metal removing operations in order to achieve parts with desired shapes, dimensions, and surface finish quality. The machining operations can be classified under two major categories: cutting and grinding processes. The cutting operations are used to remove material from the blank. The subsequent grinding operations provide a good surface finish and precision dimensions to the part. The most common cutting operations are *turning*, *milling*, and *drilling* followed by special operations such as *boring, broaching, hobing, shaping*, and *form cutting*. However, all metal cutting operations share the same principles of mechanics, but their geometry and kinematics may differ from each other. The mechanics of cutting and the specific analysis for a variety of machining operations and tool geometries are not widely covered in this text. Instead, a brief introduction to the fundamentals of cutting mechanics and a comprehensive discussion of the mechanics of milling operations are presented. Readers are referred to established metal cutting texts authored by Armarego and Brown [2], Shaw [3], and Oxley [4] for detailed treatment of the machining processes.

2.2 MECHANICS OF ORTHOGONAL CUTTING

Although the most common cutting operations are three dimensional and geometrically complex, the simple case of two-dimensional orthogonal cutting is used to explain the general mechanics of metal removal. In orthogonal cutting, the material is removed by a cutting edge that is perpendicular to the direction of relative tool–workpiece motion. The mechanics of more complex three-dimensional oblique cutting operations are usually evaluated by geometrical and kinematic transformation models applied to the orthogonal cutting process. Schematic representations of orthogonal and oblique cutting processes are shown in Figure 2.1. The orthogonal cutting resembles a shaping process with a straight tool whose cutting edge is perpendicular to the cutting velocity (V). A metal chip with a width of cut (b) and depth of cut (h) is sheared away from the workpiece. In orthogonal cutting, the cutting is assumed to be uniform

along the cutting edge; therefore it is a two-dimensional plane strain deformation process without side spreading of the material. Hence, the cutting forces are exerted only in the directions of velocity and uncut chip thickness, which are called tangential (F_t) and feed forces (F_f). However, in oblique cutting, the cutting edge is oriented with an inclination angle (i) and the additional third force acts in the radial direction (F_r).

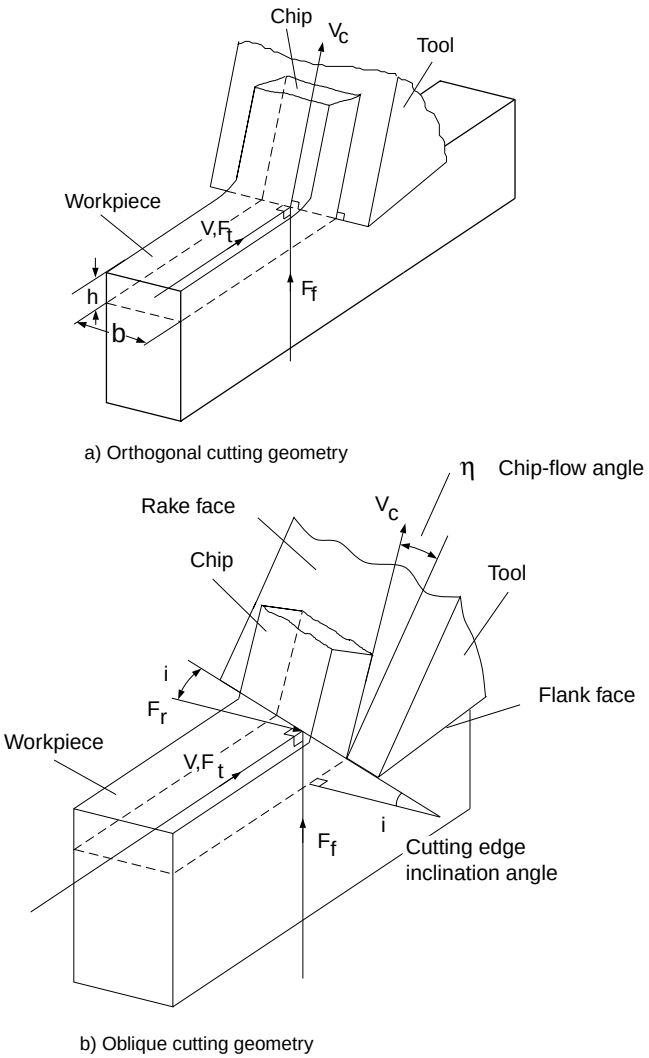

Figure 2.1: Geometries of orthogonal and oblique cutting processes.

There are three deformation zones in the cutting process as shown in the cross-sectional view of the orthogonal cutting (see Fig. 2.2). As the edge of the tool penetrates into the workpiece, the material ahead of the tool is sheared over the primary shear zone to form a chip. The sheared material, the chip, partially deforms and moves along the rake face of the tool, which is called the secondary deformation zone. The friction area, where the flank of the tool rubs the newly machined surface, is called the tertiary zone. The chip initially sticks to the rake face of the tool, which is called the *sticking region*. The friction stress is approximately equal to the yield shear stress of the material at the sticking zone where the chip moves over a material stuck on the rake face of the tool. The chip stops sticking and starts sliding over the rake face with a constant *sliding friction* coefficient. The chip leaves the tool, losing contact with the rake face of the tool. The length of the contact zone depends on the cutting speed, tool geometry, and material properties. There are basically two types of assumptions in the analysis of the primary shear zone. Merchant [5] developed an orthogonal cutting model by assuming the shear zone to be a thin plane. Others, such as Lee and Shaffer [6] and Palmer and Oxley [7], based their analysis on a thick shear deformation

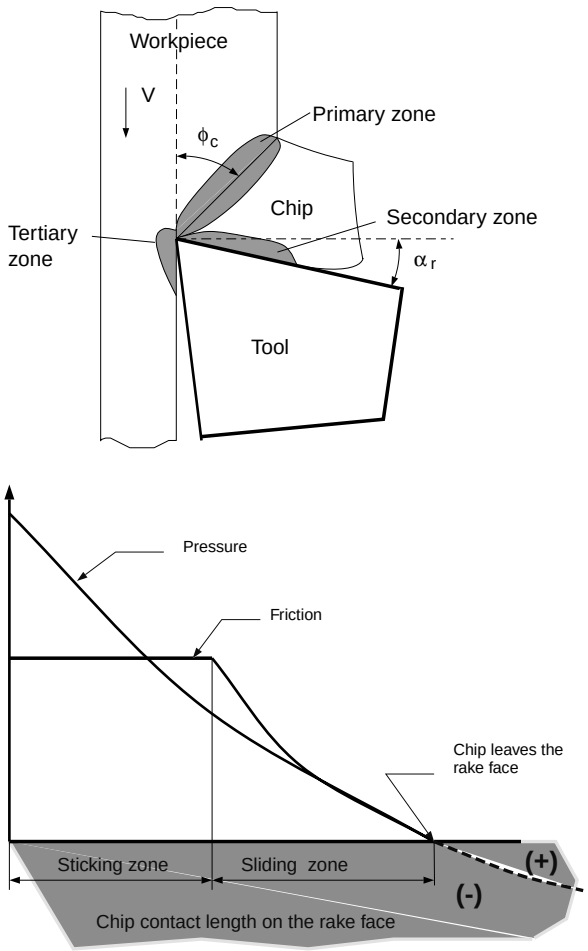

Figure 2.2: Deformation zones and distribution of load on the rake face. The tool experiences compression stress under the chip contact zone (−) and tensile stresses (+) after the chip leaves the tool.

zone, proposing "shear angle prediction" models in accordance with the laws of plasticity. In this text, the primary shear deformation zone is assumed to be a thin zone for simplification.

The deformation geometry and the cutting forces are shown on the cross-sectional view of the orthogonal cutting process (see Fig. 2.3). It is assumed that the cutting edge is sharp without a chamfer or radius and that the deformation takes place at the infinitely thin shear plane. The shear angle ϕ_c is defined as the angle between the direction of the cutting speed (V) and the shear plane. It is further assumed that the shear stress (τ_s) and the normal stress (σ_s) on the shear plane are constant; the resultant force (F) on the chip, applied at the shear plane, is in equilibrium to the force (F) applied to the tool over the chip–tool contact zone on the rake face; an average constant friction is assumed over the chip–rake face contact zone. From the force equilibrium, the resultant force (F) is formed from the feed (F_f) and tangential (F_t) cutting forces:

$$F = \sqrt{F_t^2 + F_f^2}. \tag{2.1}$$

The feed force (or thrust force) is in the direction of uncut chip thickness and the tangential cutting force (or power force) is in the direction of cutting velocity. The cutting forces acting on the tool will have equal amplitude but opposite directions with respect to the forces acting on the chip. The mechanics of orthogonal cutting for two deformation zones are shown as follows:

Primary Shear Zone. The shear force (F_s) acting on the shear plane is derived from the geometry:

$$F_s = F\cos(\phi_c + \beta_a - \alpha_r), \tag{2.2}$$

where β_a is average friction angle between the tool's rake face and the moving chip, and α_r is the rake angle of the tool. The shear force can also be expressed

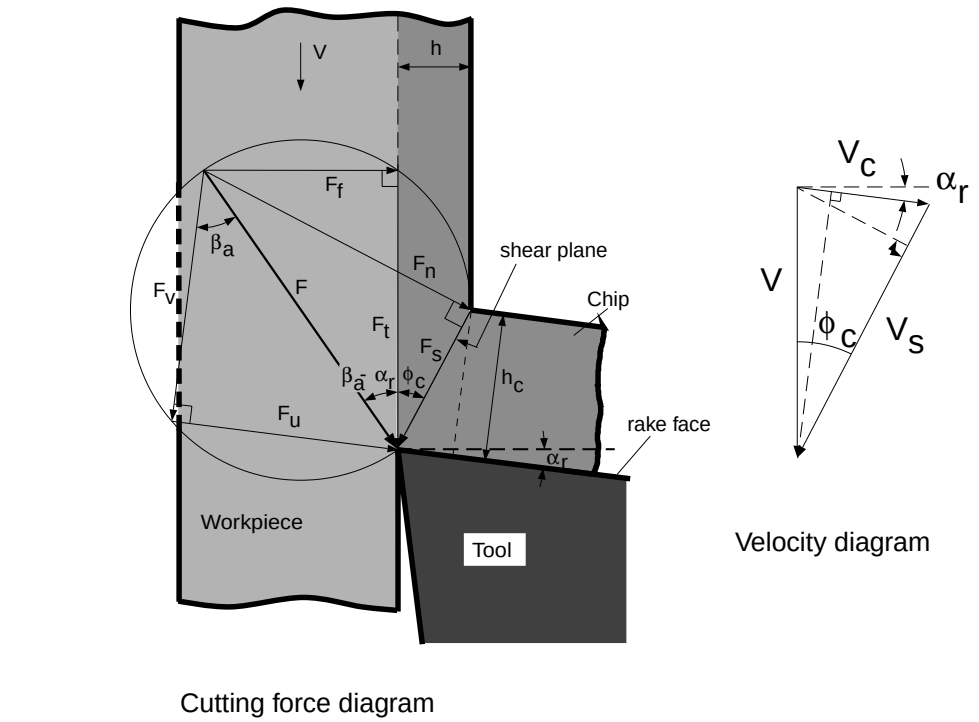

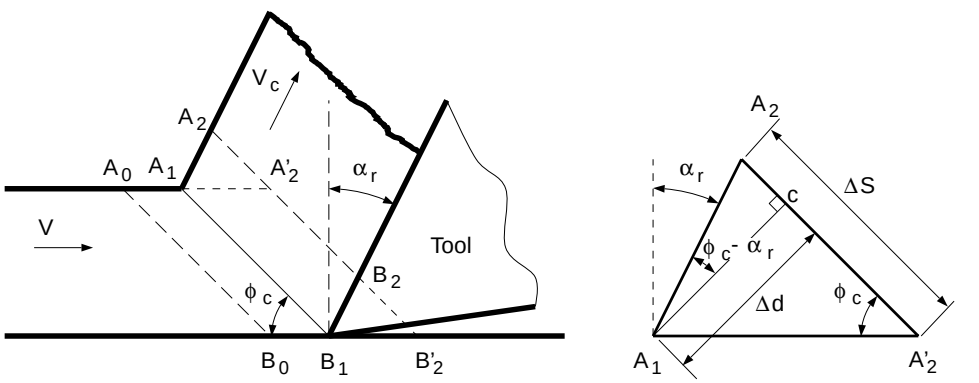

Figure 2.3: Mechanics of orthogonal cutting.

as a function of the feed and tangential cutting forces:

$$F_s = F_t \cos \phi_c - F_f \sin \phi_c. \tag{2.3}$$

Similarly, the normal force acting on the shear plane is found to be

$$F_n = F \sin(\phi_c + \beta_a - \alpha_r) \tag{2.4}$$

or

$$F_n = F_t \sin\phi_c + F_f \cos\phi_c. \tag{2.5}$$

With the assumption of uniform stress distribution on the shear plane, the shear stress (τ_s) is found to be

$$\tau_s = \frac{F_s}{A_s}, \tag{2.6}$$

where the shear plane area (A_s) is

$$A_s = b\frac{h}{\sin\phi_c} \tag{2.7}$$

and b is the width of cut (or depth of cut in turning), h is the uncut chip thickness, and (ϕ_c) is the shear angle between the direction of cutting speed (V) and the shear plane. The normal stress on the shear plane (σ_s) is

$$\sigma_s = \frac{F_n}{A_s}. \tag{2.8}$$

The cutting velocity (V) is resolved into two components (see the velocity diagram shown in Fig. 2.3). The material is sheared away from the workpiece with the shear velocity (V_s). From the velocity hodograph shown, we have

$$V_s = V\frac{\cos\alpha_r}{\cos(\phi_c - \alpha_r)}. \tag{2.9}$$

The shear power spent in the shear plane is

$$P_s = F_s \cdot V_s, \tag{2.10}$$

which is converted into heat. The corresponding temperature rise on the shear plane (T_s) is

$$P_s = m_c c_s (T_s - T_r), \tag{2.11}$$

where m_c is the metal removal rate [kg/sec], c_s is the specific coefficient of heat for the workpiece material [Nm/kg°C], and T_r is the shop temperature. Metal removal rate is found from the cutting process conditions,

$$\left.\begin{aligned} m_c &= Q_c\rho, \\ Q_c &= bhV \quad [\mathrm{m^3/s}], \end{aligned}\right\} \tag{2.12}$$

where ρ[kg/m^3] is the specific density of the workpiece material. The shear plane temperature (T_s) can be calculated from Eqs. (2.9) to (2.12):

$$T_s = T_r + \frac{P_s}{m_c c_s}. \tag{2.13}$$

The formulation given above considers that the entire plastic deformation takes place only at the shear plane and that all the heat is also consumed at the shear plane. This assumption is shown to overestimate the temperature prediction proposed by Boothroyd [8], who considered that some of the

plastic deformation takes place over a shear zone of finite thickness and that some of the heat is dissipated to the work material and the chip, away from the thin shear plane. Oxley [4] used the following modified temperature prediction:

$$T_s = T_r + \lambda_h(1-\lambda_s)\frac{P_s}{m_c c_s} \tag{2.14}$$

where λ_h ($0 < \lambda_h \leq 1$) is a factor that considers the plastic work done outside the thin shear zone, and λ_s is the proportion of the heat conducted into the work material. For a plain carbon steel, an average value for $\lambda_h \approx 0.7$ can be assumed [9]. The heat conducted into the work material is evaluated with the following experimentally evaluated empirical equation [4]:

$$\begin{aligned} \lambda_s &= 0.5 - 0.35\log(R_T \tan\phi_c), \quad \text{for} \quad 0.04 \leq R_T \tan\phi_c \leq 10, \\ \lambda_s &= 0.3 - 0.15\log(R_T \tan\phi_c), \quad \text{for} \quad R_T \tan\phi_c \geq 10, \end{aligned} \tag{2.15}$$

where ϕ_c is the shear angle and R_T is a nondimensional thermal number given by

$$R_T = \frac{\rho c_s V h}{c_t}, \tag{2.16}$$

where c_t is the thermal conductivity of the work material with units [W/(m°C)]. Note also that the heat transmitted to the work material can not be more than the total energy generated, and a negative influx of the heat into the shear plane is not possible ($0 \leq \lambda_s \leq 1$).

The shear plane length L_c is found from the chip deformation geometry,

$$L_c = \frac{h}{\sin\phi_c} = \frac{h_c}{\cos(\phi_c - \alpha_r)}. \tag{2.17}$$

The chip compression ratio (r_c) is the ratio of the uncut chip thickness over the deformed (h_c) one,

$$r_c = \frac{h}{h_c}. \tag{2.18}$$

The shear angle is found from the geometry as a function of rake angle and the chip compression ratio,

$$\phi_c = \tan^{-1}\frac{r_c \cos\alpha_r}{1 - r_c \sin\alpha_r}. \tag{2.19}$$

The shear strains and strain rates in metal cutting are significantly higher than those found from standard tensile tests and metal forming operations. The geometry of a deformed chip is shown in Figure 2.3. Assume that an undeformed chip section $A_0B_0A_1B_1$ is moving with workpiece velocity V. The workpiece material is deformed plastically at the shear plane (B_1A_1), and the cut chip slides over the rake face with a chip velocity V_c. After Δt shearing time, the uncut metal strip $A_0B_0B_1A_1$ becomes a chip with a geometry of $A_1B_1B_2A_2$. Hence, the chip is shifted from expected position of $B_2'A_2'$ to the deformed position B_2A_2 due to shearing in the shear plane with a shear angle of ϕ_c. Due

to plane strain deformation, $A'_2A_2 = B'_2B_2$. The shear strain (γ_s) is defined as the ratio of deformation ($\Delta s = A'_2A_2$) over the nominal distance between the deformed and undeformed planes ($\Delta d = A_1C$),

$$\gamma_s = \frac{\Delta s}{\Delta d} = \frac{\overline{A_2A'_2}}{\overline{A_1C}} = \frac{\overline{A'_2C}}{\overline{A_1C}} + \frac{\overline{CA_2}}{\overline{A_1C}} = \cot\phi_c + \tan(\phi_c - \alpha_r).$$

By rearranging, the shear strain can be expressed as

$$\gamma_s = \frac{\cos\alpha_r}{\sin\phi_c \cos(\phi_c - \alpha_r)}. \tag{2.20}$$

The shear strain rate is

$$\gamma'_s = \frac{\gamma_s}{\Delta t}.$$

Assuming that the shear zone increment is Δs and that the thickness of shear deformation zone is Δd, the shear strain and shear velocity can be defined as $\gamma_s = \Delta s/\Delta d$ and $V_s = \Delta s/\Delta t$, respectively. The shear strain rate is then defined as

$$\gamma'_s = \frac{V_s}{\Delta d} = \frac{V\cos\alpha_r}{\Delta d\cos(\phi_c - \alpha_r)}. \tag{2.21}$$

Since the shear zone thickness Δd is extremely small in cutting, Eq. 2.21 indicates the presence of very high shear strain rates. Especially when the shear zone is assumed to be a plane with zero thickness, the strain rate becomes infinite, which can not be true. However, the thin shear plane approximation is useful for the macromechanics analysis of metal cutting. For practical and approximate predictions, the thickness of the shear zone can be approximated as a fraction of the shear plane length (i.e., $\Delta d \approx 0.15$–$0.2\,L_c$). For more accurate analysis, the shear zone thickness must be evaluated by freezing the machining process with a quick stop test and measuring the zone thickness with a scanning electron microscope (SEM).

Secondary Shear Zone. There are two components of the cutting force acting on the rake face of the tool (Fig. 2.3); the normal force F_v,

$$F_v = F_t\cos\alpha_r - F_f\sin\alpha_r, \tag{2.22}$$

and the friction force F_u on the rake face,

$$F_u = F_t\sin\alpha_r + F_f\cos\alpha_r. \tag{2.23}$$

In the orthogonal cutting analysis shown here, it is assumed that the chip is sliding on the tool with an average and constant friction coefficient of μ_a. In reality, the chip sticks to the rake face for a short period and then slides over the rake face with a constant friction coefficient [10]. The average friction coefficient on the rake face is given as

$$\mu_a = \tan\beta_a = \frac{F_u}{F_v}. \tag{2.24}$$

The friction angle β_a can alternatively be found from the tangential and feed forces,

$$\tan(\beta_a - \alpha_r) = \frac{F_f}{F_t}. \quad \rightarrow \quad \beta_a = \alpha_r + \tan^{-1}\frac{F_f}{F_t}. \tag{2.25}$$

The deformed chip slides on the rake face of the tool with the velocity of

$$V_c = r_c V = \frac{\sin\phi_c}{\cos(\phi_c - \alpha_r)} V. \tag{2.26}$$

Friction power spent on the tool chip contact face is

$$P_u = F_u V_c. \tag{2.27}$$

The total power consumed in cutting is the sum of energy spent in the shear and friction zones:

$$P_t = P_s + P_u. \tag{2.28}$$

From the equilibrium of cutting forces and the velocities, the total power is also equal to the cutting power drawn from the spindle motor:

$$P_t = F_t V. \tag{2.29}$$

The friction power increases the temperature of tool and chip. As can be seen from Eq. (2.27) if the velocity is increased, the friction power and thus the temperature of the tool increase. Excessive heat will cause undesirable high temperature in the tool, which leads to softening of the tool material and its accelerated wear and breakage. However, the production engineer desires an increased cutting velocity to obtain a high metal removal rate (Eq. 2.12) for productivity gains. The manufacturing researchers' challenge has been to decrease the cutting force F_u and move the heat toward the chip with better tool geometry design and to develop heat-resistant tool materials that can preserve their hardness at elevated temperatures. Although the prediction of the temperature distribution at the tool–chip interface is rather complex, the following simplified analysis is still useful for metal cutting engineers.

The friction power consumed at the tool chip interface (Eq. 2.27) is converted into heat via

$$P_u = m_c c_s \Delta T_c, \tag{2.30}$$

where ΔT_c is the average temperature rise in the chip. Boothroyd [8] and Stephenson [11] assumed a constant sticking friction load with a constant rectangular plastic zone at the tool–chip interface. The experimental temperature measurement and assumed plastic deformation zone led to the following empirical temperature relationship [4]:

$$\log\left(\frac{\Delta T_m}{\Delta T_c}\right) = 0.06 - 0.195\delta\sqrt{\frac{R_T h_c}{l_t}} + 0.5\log\left(\frac{R_T h_c}{l_t}\right), \tag{2.31}$$

where ΔT_m is the maximum temperature rise of the chip at the rake face–chip interface, which has a total contact length of l_t. The nondimensional number δ is the ratio of the plastic layer thickness over the deformed chip thickness (h_c) on the tool rake face–chip interface. The average temperature rise (T_{int}) at the rake face–chip interface is given by

$$T_{int} = T_s + \lambda_{int} \Delta T_m, \tag{2.32}$$

where T_s is the average shear plane temperature and λ_{int} (i.e., $\approx$0.7) is an empirical correction factor that accounts for temperature variations along the chip–tool contact zone. For an accurate analysis, both the plastic layer thickness (δh_c) and l_t must be measured with a microscope that has a large magnification (such as a SEM). Our experiments indicated that the thickness of the plastic layer on the rake face is observed to be between 5 and 10% of the deformed chip thickness ($\delta / h_c \approx 0.05$–$0.1$). The contact length can be estimated approximately by assuming that the resultant cutting force acts in the middle of the contact length and parallel to the stress-free chip boundary. From the geometry of orthogonal cutting (Fig. 2.3), the chip–rake face contact length can be approximately predicted as

$$l_t = \frac{h \sin(\phi_c + \beta_a - \alpha_r)}{\sin \phi_c \cos \beta_a}. \tag{2.33}$$

The prediction of temperature distribution at the tool–chip interface is very important in determining the maximum speed that gives the most optimal material removal rate without excessive tool wear. The binding materials within the cutting tools may be weakened or diffused to the moving chip material at their critical diffusion or melting temperature limits. The fundamental machinability study requires the identification of a maximum cutting speed value that corresponds to the critical temperature limit where the tool wears rapidly. By using the approximate solutions summarized above, one can select a cutting speed that would correspond to a tool–chip interface temperature (T_{int}) that lies just below the diffusion and melting limits of materials present in a specific cutting tool. The detailed and fundamental scientific and experimental treatment of the cutting process is covered in Oxley [4].

It is difficult to predict the shear angle and stress in the shear plane and the average friction coefficient on the rake face using the standard material properties obtained from tensile and friction tests. For an accurate and realistic modeling, such fundamental parameters are identified from orthogonal cutting tests, where the deformed chip thickness and feed and tangential cutting forces are measured using cutting tools with a range of rake angles. The influence of uncut chip thickness and cutting speed is also considered by conducting experiments over a wide range of feeds and cutting speeds.

The relationships shown in Table 2.1 are identified from statistical analysis of more than 180 orthogonal cutting tests conducted using tungsten carbide (WC) cutting tools and Ti_6Al_4V titanium alloy work material. A set of turning experiments resembling orthogonal cutting was conducted on titanium

tubes (Ti_6Al_4V) with tools of different rake angles at different feeds and cutting speeds. The diameter of the tube was 100 mm and the cutting speed range was 2.6 to 47 m/min. Cutting forces in the tangential (F_t) and feed (F_f) directions were measured with a force dynamometer. Two sample orthogonal cutting test results are shown in Figure 2.4. Small steps in cutting conditions were used to increase the reliability of the measured forces. It should be noted that the measured forces may include both the forces due to shearing and a tertiary deformation process "ploughing" or "rubbing" at the flank of the cutting edge. Thus the measured force components are expressed as a superposition of shearing and edge forces:

TABLE 2.1. Orthogonal Cutting Data Base for Titanium Alloy Ti_6Al_4V

$\tau_s = 613$ (MPa)
$\beta_a = 19.1 + 0.29\alpha_r$ (deg)
$r_c = C_o h^{C_1}$
$C_o = 1.755 - 0.028\alpha_r$
$C_1 = 0.331 - 0.0082\alpha_r$
$K_{te} = 24$ (N/mm)
$K_{fe} = 43$ (N/mm)

$$\begin{aligned} F_t &= F_{tc} + F_{te}, \\ F_f &= F_{fc} + F_{fe}. \end{aligned} \tag{2.34}$$

The tests have been repeated a number of times at different feeds and cutting speed to ensure the statistical reliability of measurements. The edge forces are obtained by extrapolating the measured forces to zero chip thickness. It can be seen that the edge forces do not vary significantly with cutting speeds for the particular titanium alloy used here. The average edge force coefficients K_{te} and K_{fe} represent the rubbing forces per unit width. The chip compression ratio (r_c), shear stress τ_s, shear angle ϕ_c, and friction angle β_a (Table 2.1) are calculated from the measured "cutting" component of the forces and the cutting ratio by applying the orthogonal cutting theory presented above.

2.3 MECHANISTIC MODELING OF CUTTING FORCES

Orthogonal cutting mechanics are not directly applicable to many practical cutting tools with corner radius, side cutting edge angle, and chip breaking grooves. It is more practical to carry out a few experiments to identify constant parameters of the tool geometry–workpiece material pair to model existing cutting tools. However, it must be noted that for a tool design and analysis of a particular metal cutting process, oblique (i.e., three-dimensional) cutting mechanics and plasticity analysis are still necessary, and this is covered in Section 2.5.

As an example of mechanistic modeling, let us take the case of orthogonal cutting. We can extend the idea of model building to other cutting processes that are not orthogonal. In the previous section, the shearing force is formulated as a function of measured feed and tangential cutting forces in the orthogonal cutting. The shear force can be expressed as a function of shear stress and shear angle (Eqs. 2.6 and 2.7):

$$F_s = \tau_s b \frac{h}{\sin \phi_c}. \tag{2.35}$$

From Eqs. (2.2) and (2.35), the resultant cutting force (F) can be expressed in

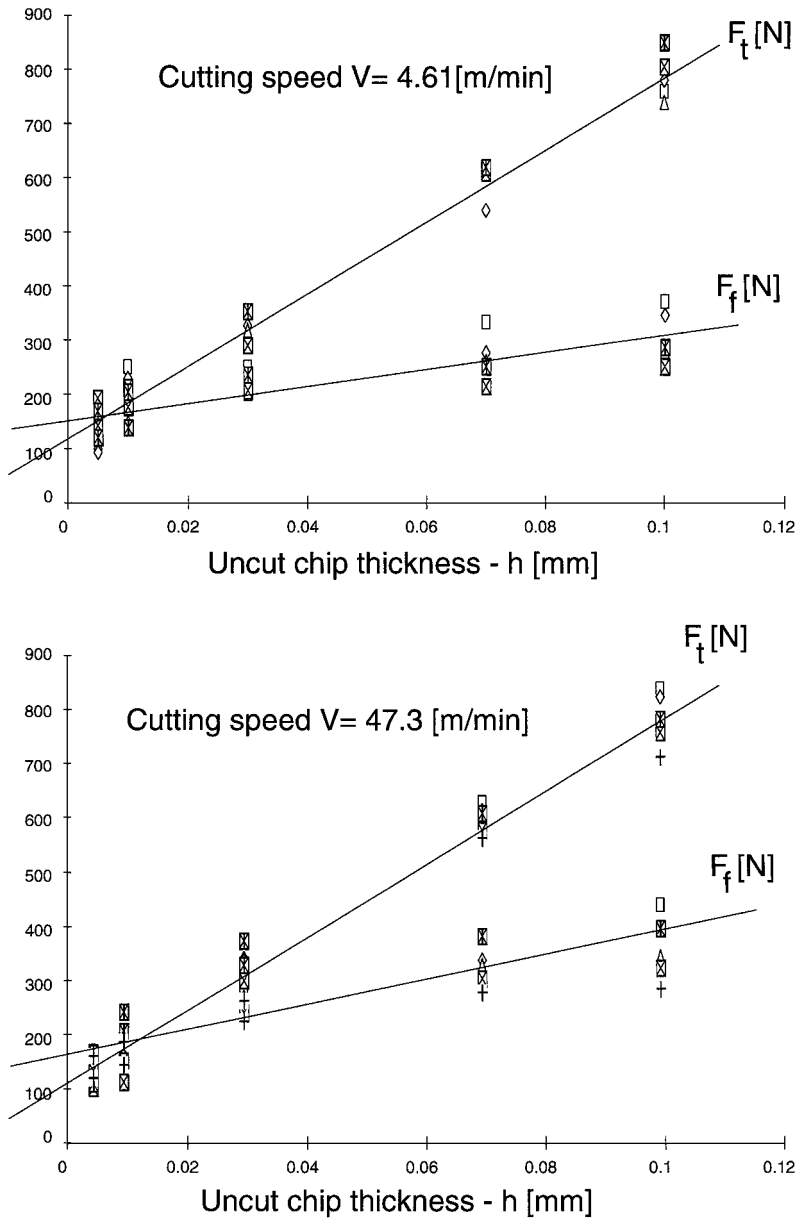

Figure 2.4: Cutting forces measured during orthogonal turning of Ti_6Al_4V tubes with tungsten carbide tools.

terms of shear stress, friction and shear angles, width of cut, and feed rate:

$$F = \frac{F_s}{\cos(\phi_c + \beta_a - \alpha_r)} = \tau_s bh \frac{1}{\sin\phi_c \cos(\phi_c + \beta_a - \alpha_r)}. \tag{2.36}$$

The tangential and feed forces can be expressed in terms of resultant force:

$$\left.\begin{aligned} F_t &= F\cos(\beta_a - \alpha_r), \\ F_f &= F\sin(\beta_a - \alpha_r). \end{aligned}\right\} \tag{2.37}$$

Substituting Eq. (2.36) into Eq. (2.37), we can find the measured main cutting forces as functions of tool geometry and the cutting conditions (i.e., uncut chip thickness (h) and width of cut (a)) and process- and material-dependent terms (τ_s, β_a, ϕ_c, α_r):

$$F_t = bh\left[\tau_s \frac{\cos(\beta_a - \alpha_r)}{\sin\phi_c \cos(\phi_c + \beta_a - \alpha_r)}\right]. \tag{2.38}$$

Similarly the feed force is

$$F_f = bh\left[\tau_s \frac{\sin(\beta_a - \alpha_r)}{\sin\phi_c \cos(\phi_c + \beta_a - \alpha_r)}\right]. \tag{2.39}$$

In metal cutting literature the cutting parameter called *specific cutting pressure* or *tangential cutting force coefficient* (K_t) is defined as

$$K_t\,[\mathrm{N/mm^2}] = \tau_s \frac{\cos(\beta_a - \alpha_r)}{\sin\phi_c \cos(\phi_c + \beta_a - \alpha_r)} \tag{2.40}$$

and the feed force constant (K_f) as

$$K_f\,[\mathrm{N/mm^2}] = \tau_s \frac{\sin(\beta_a - \alpha_r)}{\sin\phi_c \cos(\phi_c + \beta_a - \alpha_r)}. \tag{2.41}$$

It is also customary to use another convention for cutting constants, where the feed force is assumed to be proportional to the tangential force with a ratio of

$$K_f = \frac{F_f}{F_t} = \tan(\beta_a - \alpha_r), \tag{2.42}$$

where K_f is dimensionless in this form. As can be seen from the definition (Eq. 2.40), the specific cutting pressure is a function of the yield shear stress of the workpiece (τ_s) material during cutting, the shear angle (ϕ_c), tool geometry (i.e., rake angle α_r), and the friction between the tool and the chip (β_a). In Eq. (2.40), only the tool geometry is known beforehand. The friction angle depends on the lubrication used, the tool–chip contact area, and the tool and workpiece materials. An accurate, analytical shear angle prediction remains the subject of continuing research. Previous research results are still insufficient to be used in predicting the shear angles accurately. The shear stress in the shear plane is also still in question with the present knowledge of the cutting process. If the shear plane is assumed to be a thick zone, which is more realistic than having a thin shear plane, there will be a work hardening, and the shear stress will be larger than the workpiece material's original yield shear stress measured from pure torsion or tensile tests. The temperature variation in the shear and the friction zones will also affect the hardness of the workpiece material; therefore the shear stress in the primary deformation zone will vary. The shear yield stress varies as a function of chip thickness as well due to varying strain hardening of the material being machined. Hence, it is customary to define the cutting forces mechanistically as a function of cutting conditions

(i.e., b and h) and the cutting constants (K_{tc}) and (K_{fc}):

$$\left.\begin{aligned} F_t &= K_{tc} bh + K_{te} b, \\ F_f &= K_{fc} bh + K_{fe} b. \end{aligned}\right\} \tag{2.43}$$

The cutting constants (K_{tc}, K_{fc}), and the edge coefficients that do not contribute to the shearing (K_{te}, K_{fe}), are directly calibrated from metal cutting experiments for a tool–workpiece pair. Note that the edge coefficients change as the cutting tool wears or experiences chipping. It should be also noted that in order to take the influence of the chip thickness on the friction and shear angles, and the yield shear stress, the specific cutting pressure (K_t) and ratio (K_f) are sometimes expressed as nonlinear functions of uncut chip thickness:

$$\left.\begin{aligned} K_t &= K_T h^{-p}, \\ K_f &= K_F h^{-q}, \end{aligned}\right\} \tag{2.44}$$

where p and q are cutting force constants determined from the cutting experiments at different feed rates. Equation (2.44) represents basic nonlinearity in the cutting force expressions. This form is used when the edge forces are neglected in the mechanistic models. It must be noted that some work materials exhibit different yield stress and friction coefficient at different speeds, which lead to the speed dependency of cutting constants. The mechanistic cutting constant equation (2.44) can be extended to include cutting speed as a variable.

Example. The cutting conditions for turning an AISI-1045 steel workpiece are set as follows: depth of cut $b = 2.54$ mm; feed rate $c = 0.2$ mm/rev; spindle speed $n = 350$ rev/min; workpiece diameter = 100. mm; tool's rake angle $\alpha_r = +5^\circ$. Specific mass of the steel $\rho = 7{,}800$ kg/m^3; specific heat coefficient of steel $c_s = 470$ Nm/kg$^\circ$C; thermal conductivity $c_t = 28.74$ [W/m$^\circ$C]. The following measurements are observed from the experiment: deformed chip thickness $h_c = 0.44$ mm, feed force $F_f = 600$ N, tangential force $F_t = 1{,}200$ N. Assuming that the turning is an orthogonal metal cutting process, the following values are evaluated:

Resultant cutting force	$F = \sqrt{F_t^2 + F_f^2} = 1342.$ N
Chip ratio	$r_c = \frac{h}{h_c} = 0.4545$
Shear angle	$\phi_c = \tan^{-1} \frac{r_c \cos \alpha_r}{1 - r_c \sin \alpha_r} = 25^\circ$
Friction angle	$\beta_a = \alpha_r + \tan^{-1} \frac{F_f}{F_t} = 31.6^\circ$
Friction coefficient	$\mu_a = \tan \beta_a = 0.6144$
Shearing force	$F_s = F \cos(\phi_c + \beta_a - \alpha_r) = 833.5$ N
Shear plane area	$A_s = b \frac{h}{\sin \phi_c} = 1.2$ mm^2
Shearing stress	$\tau_s = \frac{F_s}{A_s} = 693.4$ MPa
Normal force on the shear plane	$F_n = F \sin(\phi_c + \beta_a - \alpha_r) = 1051.7$ N
Normal stress on the shear plane	$\sigma_s = \frac{F_n}{A_s} = 876.43$ MPa

Cutting speed	$V = \pi Dn = 110$ m/min
Shearing velocity	$V_s = V\frac{\cos\alpha_r}{\cos(\phi_c - \alpha_r)} = 116.6$ m/min $= 1.9436$ m/s
Shearing power	$P_s = F_s V_s = 1{,}620$ W
Metal removal rate	$m_c = Q_c\rho = bhV\rho = 7.2644 \cdot 10^{-3}$ kg/s
Nondimensional thermal number	$R_T = \frac{\rho c_s V h}{c_t} = 45.78, \quad R_T \tan\phi_c = 21.34 > 10$
Scale of heat conducted into work	$\lambda_s = 0.3 - 0.15\log(R_T \tan\phi_c) = 0.1$
Shear plane temperature	$T_s = T_r + \lambda_h(1-\lambda_s)\frac{P_s}{m_c c_s} = 20 + 299 = 319^\circ$C, $(\lambda_h \approx 0.7)$
Friction force	$F_u = F\sin\beta_a = 703.2$ N
Normal force	$F_v = F\cos\beta_a = 1143$ N
Chip velocity	$V_c = r_c V = 50$ m/min $= 0.8333$ m/s
Friction power	$P_u = F_u V_c = 586$ W
Chip contact length	$l_t = \frac{h\sin(\phi_c + \beta_a - \alpha_r)}{\sin\phi_c \cos\beta_a} = 0.435$ mm
Total cutting power drawn	$P_t = P_u + P_s = 2{,}200$ W
Specific cutting pressure	$K_t = \frac{F_t}{bh} = 2{,}362.$ N/mm^2
Cutting force ratio	$K_f = \frac{F_f}{F_t} = 0.5$

2.4 THEORETICAL PREDICTION OF SHEAR ANGLE

The evaluation of shear angle, shear stress, and average friction coefficient from orthogonal metal cutting tests was summarized in the previous sections. There have been many attempts in predicting the shear angle theoretically, without relying on metal cutting experiments. Some of the most fundamental models, which assume a perfect rigid plastic workpiece material without any strain hardening, are briefly presented in this section. These models assume that the shear plane is thin; that the shear stress in the shear plane is equivalent to the yield shear stress of the material; and that the average friction is found from friction tests between the tool and workpiece materials, leaving only the shear angle as unknown. There have been two fundamental approaches to predict the shear angle as follows.

Maximum Shear Stress Principle

Krystof [12] proposed a shear angle relation based on the maximum shear stress principle (i.e., shear occurs in the direction of maximum shear stress). The resultant force makes an angle $(\phi_c + \beta_a - \alpha_r)$ with the shear plane (see Fig. 2.3), and the angle between the maximum shear stress and the principal stress (i.e., the resultant force) must be $\pi/4$. Therefore, the following shear angle relation is obtained:

$$\phi_c = \frac{\pi}{4} - (\beta_a - \alpha_r). \tag{2.45}$$